Temperature-Dependent Supramolecular Isomerism of Lutetium-Aminoterephthalate Metal-Organic Frameworks

Synthesis, Crystallography, and Physical Properties

Dikhtiarenko, Alla; Serra-Crespo, Pablo; Castellanos Ortega, S.; Pustovarenko, A.; Mendoza-Merono, Rafael; García-Granda, Santiago; Gascon, J.

DOI
10.1021/acs.cgd.6b00274

Publication date
2016

Document Version
Accepted author manuscript

Published in
Crystal Growth & Design

Citation (APA)
Dikhtiarenko, A., Serra-Crespo, P., Castellanos Ortega, S., Pustovarenko, A., Mendoza-Merono, R., García-Granda, S., & Gascon, J. (2016). Temperature-Dependent Supramolecular Isomerism of Lutetium-Aminoterephthalate Metal-Organic Frameworks: Synthesis, Crystallography, and Physical Properties. *Crystal Growth & Design*, *16*(10), 5636-5645. https://doi.org/10.1021/acs.cgd.6b00274

Temperature-Dependent Supramolecular Isomerism of Lutetium-Aminoterephthalate Metal-Organic Frameworks: Synthesis, Crystallography and Physical Properties

Journal:	*Crystal Growth & Design*
Manuscript ID	cg-2016-00274f.R2
Manuscript Type:	Article
Date Submitted by the Author:	n/a
Complete List of Authors:	Dikhtiarenko, Alla; Delft University of Technology, Chemical Engineering/Catalysis Engineering Serra-Crespo, Pablo; Delft University of Technology, Radiation and Isotopes for Health / Radiation Science & Technology Castellanos, Sonia; Delft University of Technology, Chemical Engineering/Catalysis Engineering Pustovarenko, Alexey; Technische Universiteit Delft, Chemical Engineering Mendoza-Meroño, Rafael; Universidad de Oviedo García-Granda, Santiago; Universidad de Oviedo, Departamento de Quımica Fısica y Analıtica Gascon, Jorge; Delft University of Technology, Chemical Engineering Department / Catalysis Engineering Section

Temperature-Dependent Supramolecular Isomerism of Lutetium-Aminoterephthalate Metal-Organic Frameworks: Synthesis, Crystallography and Physical Properties.

A. Dikhtiarenko[1, ‡], P. Serra-Crespo[2, ‡,], S. Castellanos[1], A. Pustovarenko[1], R. Mendoza-Meroño[3], S. García-Granda[3] and J. Gascon[1,*]*

[1] Catalysis Engineering, ChemE, Delft University of Technology, Julianalaan 136, 2628 BL, Delft, The Netherlands.

[2] Radiation and Isotopes for Health, Radiation Science and Technology, Delft University of Technology, Mekelweg 15, 2629 JB, Delft, The Netherlands

[3] Departamento de Química Física y Analítica, Universidad de Oviedo—CINN, Julian Claveria s/n, 33006 Oviedo, Spain

KEYWORDS: Lutetium, metal-organic framework, temperature-dependent supramolecular isomerism, gas adsorption, luminescence

ABSTRACT

Three supramolecular isomers of lutetium metal-organic framework, $\{Lu_2(H_2O)_4(ATA)_3\cdot 4H_2O\}_n$ (**Lu-ATA@RT**), $\{Lu_2(H_2O)_2(C_3H_7NO)_2(ATA)_3\}_n$ (**Lu-ATA@100**) and $\{Lu_2(C_3H_7NO)(ATA)_3\}_n$ (**Lu-ATA@150**), have been obtained from the reaction of $Lu(NO_3)_3\cdot 6H_2O$ with 2-aminoterephthalic acid (ATA) at different temperatures. The resulting structures of Lu-ATA MOFs depend on the temperature applied during the synthesis, revealing a temperature-susceptible supramolecular isomerism. Single-crystal X-ray diffraction analyses suggest that new compounds with formula $\{Lu_2(S)_x(ATA)_3\}_n$ (S = solvent: H_2O, DMF) display different three-dimensional architectures which consist on dinuclear lutetium building units. The supramolecular isomer **Lu-ATA@RT**, formed at room temperature, has a pcu-net topology while its double interpenetrated analogue, **Lu-ATA@100**, assembles at 100 ºC under hydrothermal conditions. Hydrothermal synthesis at 150 ºC affords formation of the dense **Lu-ATA@150** cage-like framework displaying a new hexagonal-packed net topology. All Lu-ATA isomeric phases are porous and display different gas-uptake behaviour towards carbon dioxide as a function of polymeric network arrangement. The luminescent properties of Lu-ATA frameworks in solid state as well as in suspension in the presence of different solvents reveal a solvent dependent emission.

Introduction

During the past decades, the research field focused on porous materials underwent a revolution with the appearance of metal-organic frameworks (MOFs).[1-3] These porous solids constitute a subclass of three-dimensional (3D) coordination polymers formed by combination of metal ions or metal-oxygen clusters with organic ligands. These highly crystalline microporous materials have received enormous attention due to their manifold properties, with application in many different fields,[4] from gas adsorption and separation to catalysis,[5, 6] sensing and medicine.[7, 8]

In general, practical applications of MOFs are directly related to their structural features.[9-12] Therefore, the rational design of MOFs' structures at molecular as well as nano- or macro-levels is still one of the main activities in the topic.[13, 14] Polymorphism or supramolecular isomerism is becoming an increasingly important subject in the field of crystal engineering, as it may facilitate the design of porous polymeric materials with targeted physical properties.[15-17] In this context, the unique properties of MOF polymorphs, displaying both different crystal structures and identical molecular composition, allow for the derivation of structure-property relationships solely based on structural parameters or topology of the polymeric network.[18] There are various key factors governing the formation of MOFs' polymorphic forms, including reaction time, temperature, concentration of precursors, pH, solvent, modulators, and so on. For example, Shi *et al*. report two polymorphic frameworks consisted of Eu^{III}, 2,5-furandicarboxylic and oxalic acids, which formation is determined by pH of reaction solution.[19] In addition, the nature of the solvent is also an important factor that influences on the topology of resulted polymeric structure.[20] Therefore, several polymorphic forms of Pb^{II} and Cu^{II}-based MOFs were successfully obtained using different solvents or their mixtures.[21, 22] Similarly, the polymorphism of 3D MOFs was found to be instigated by modulators or structure directing agents.[23, 24] As

example, Zhu *et al*. isolated two polymorphic forms of augmented "Cu_2-paddlewheel"-based MOFs with identical compositions but different **tbo** and **pto** topologies which are strongly correlated with the nature of the structure directing modulator used for the synthesis.[25] Recently, Friščić *et al*. have highlighted the importance of *in-situ* solid-state routes for the monitoring of MOF's polymorphs formation.[26]

Although numerous individual factors[27] or their conjunction[28] affect the occurrence of polymorphic forms, temperature is the one of the most important variables.[29] In particular, the use of temperature enables to take advantages of entropic differences between alternative products.[30] As illustrated by several studies,[31-34] different polymorphic phases of MOFs can be obtained from a single reaction mixture held at different temperatures. Among them, the experimental and theoretical studies carried out on series of polymorphic La-based MOFs reveal that the kinetic metastable and thermodynamic phases could be isolated as pure products over certain temperature ranges.[35] Additionally, the temperature-dependent ground states in the energy landscape for Zn^{II}-imidazole polymorphs[36] were also discussed recently.[37] The study of polymorphism is not only important in producing novel materials with target properties but may also be helpful in developing a fundamental understanding of the factors influencing crystal growth, such as reaction temperature.

Despite the numerous MOFs reported in the last decades, the number of lutetium based MOFs is very scarce.[38, 39]

In this work, we report the syntheses, crystal structures, adsorption and fluorescence properties of three novel lutetium(III) 2-aminoterephthalate MOFs, namely **Lu-ATA@RT**, **Lu-ATA@100** and **Lu-ATA@150**. These three compounds are supramolecular isomeric forms of 3D lutetium(III) 2-aminoterephthalate framework, $\{Lu_2(S)_x(ATA)_3\}_n$ (S = solvent: H_2O, DMF; ATA

= 2-aminoterephthalic acid), which were obtained from identical staring materials in equal metal-to-ligand ratios under different temperatures.

Experimental Section

Materials and characterization methods. All starting materials were of analytical grade, obtained from Sigma-Aldrich and used without further purification.

Syntheses. The synthetic condition for **Lu-ATA@RT** (room temperature supramolecular isomer) was previously optimized (see Supporting Information). 0.1 g (0.26 mmol) of $Lu(NO_3)_3 \cdot 6H_2O$ was dissolved in 10 mL H_2O and mixed with an aqueous solution (5 mL) containing 0.14 g (0.77 mmol) of 2-aminoterephthalic acid (ATA) and 0.04 g (1.54 mmol) of LiOH under magnetic stirring. The resulting solution was allowed to complete the reaction for 1 hour at room temperature upon continuous stirring. The formed pale-yellow precipitate was separated by vacuum filtration, washed several times with distillated water and air dried. Yield, 0.14 g (99% based on Lu).

For **Lu-ATA@100** (supramolecular isomer formed at 100 °C) synthesis, a mixture containing 0.1 g (0.26 mmol) of $Lu(NO_3)_3 \cdot 6H_2O$, 0.05 g (0.3 mmol) of 2-aminoterephthalic acid (ATA), 2 mL of DMF and 8 mL of H_2O was placed after dissolution in a Teflon-lined autoclave and heated for 5 h at 100 °C in an oven under static conditions. The yellow precipitate was separated by vacuum filtration, washed several times with distillated water and air dried. Yield, 0.12 g (93% based on Lu).

The synthesis of **Lu-ATA@150** polymorph was realized using the same reagent amounts and procedures as for **Lu-ATA@100**, but the reaction was performed under hydrothermal conditions at 150 °C for 5 h yielding 0.10 g yellow-brown powdered product (90 % yield based on Lu). The

solid was separated by vacuum filtration, washed several times with distillated water and air dried.

Single crystal growth. Single crystals of **Lu-ATA@RT** were obtained by crystallization in a tetremethoxysilane (TMOS) gel containing (0.77 mmol) of 2-aminoterephthalic acid (ATA) and 0.04 g (1.54 mmol) of LiOH. When the gel is formed, the aqueous solution of $Lu(NO_3)_3 \cdot 6H_2O$ was placed as upper layer. After one week, prismatic yellow crystals of **Lu-ATA@RT** were formed in gel phase (Figure S1a, Supporting Information).

Scanning Electron Microscopy (SEM) was used to study the crystal size and morphology of the Lu-MOF polymorphs. SEM micrographs were acquired in a Philips XL20 (15–30 kV) microscope after sputtering the sample with a conductive Au layer.

Thermogravimetric analysis. Mettler-Toledo TGA/SDTA851e was used for the thermal analyses in air dynamic atmosphere at heating rate of 10 °C/min in the range of temperatures from 30 °C to 1000 °C (blank runs were performed).

CO_2 adsorption. Low-pressure adsorption isotherms of CO_2 (purity of 99.995%) were measured at 273 K in a device built by Bruker based on the volumetric technique. High-pressure adsorption isotherms of CO_2 (purity of 99.995%) were determined using the volumetric technique with an apparatus from BEL Japan (Belsorp HP). Around 0.2 g of the samples was placed in the sample container. Before every measurement, the adsorbent was pre-treated by increasing the temperature to 473 K at a rate of 10 K/min under vacuum and maintaining the temperature for 2 hours. The measurements for carbon dioxide adsorption at high pressure were carried out at 273 K for the complete series of Lu-MOF supramolecular isomers.

Diffuse reflectance ($BaSO_4$ as a white standard) and **absorption UV/Vis** spectra were collected using a Perkin–Elmer Lambda 900 spectrophotometer equipped with an integrating sphere

("Labsphere"). Steady-state emission spectra were acquired using the photospectrometer Quanta Master QM1 of Photon Technology International (PTI) provided with a 100 W Xenon lamp, a double excitation monochromator (model PTI 121 A), a sample box and an emission monochromator (model PTI 101 A) and a photon counting detector PMT (model 710).

X-ray structure determination. The single crystal X-ray diffraction data for **Lu-ATA@RT**, **Lu-ATA@100** and **Lu-ATA@150** were collected at 293 K on a an Oxford-Gemini X-ray diffractometer equipped with graphite-monochromatic Cu-Kα (λ = 1.5418 Å) and Mo-Kα (λ = 0.7107 Å) radiation. The CrysAlisPro program was used for cell refinement and data reduction. Images were collected at a 55 mm fixed crystal-detector distance, using the oscillation method, with 1° oscillation and variable exposure time per image. All the structures were solved by direct methods using the program SIR92[40] and refined by full-matrix least-squares techniques against F^2 using the SHELXTL-97[41] crystallographic software package. All non-hydrogen atoms were found from the difference Fourier maps and refined anisotropically, whereas the hydrogen atoms of the organic molecules were placed by geometrical considerations and were added to the structure factor calculations. In case of **Lu-ATA@150** structure, nitrogen atoms of amino-groups are refined isotropically. Moreover, terminal amino-groups of 2-aminoterephthalic ligand are disordered with occupancy ratio near to 0.5. For compounds **Lu-ATA@RT**, **Lu-ATA@100** and **Lu-ATA@150**, the high residual peaks and holes are observed in the vicinity of Lu^{3+}, which are normal for compounds containing heavy atoms. Absorption corrections were applied using XABS2 program.[42] The crystallographic data and structure refinement parameters for **Lu-ATA@RT**, **Lu-ATA@100** and **Lu-ATA@150** are summarized in the Table 1.

Table 1. Crystallographic parameters and refinement data for **Lu-ATA@RT**, **Lu-ATA@100** and **Lu-ATA@150** supramolecular isomers.

Compound	**Lu-ATA@RT**	**Lu-ATA@100**	**Lu-ATA@150**
Formula	$C_{24}H_{34}Lu_2N_6O_{20}$	$C_{30}H_{36}Lu_2N_8O_{16}$	$C_{27}H_{25}Lu_2N_4O_{13}$
FW /g·mol^{-1}	1076.5	1114.6	963.44
Temperature /K	296	296	300
Wavelength	CuKα (1.54180 Å)	MoKα (0.71073 Å)	MoKα (0.71073 Å)
Crystal system	triclinic	triclinic	monoclinic
Space group	*P* -1	*P* -1	*P* $2_1/a$
Unit cell dimensions			
a (Å)	10.0669(12)	8.1181(3)	20.5758(8)
b (Å)	10.3562(17)	10.2300(5)	16.6308(4)
c (Å)	10.538(2)	11.7103(5)	20.5719(8)
α (°)	103.158(17)	114.980(4)	90
β (°)	115.524(17)	99.906(3)	119.801(5)
γ (°)	92.546(12)	98.258(3)	90
Cell volume/ Å^3	952.6(3)	842.54(7)	6108.6(5)
Z	2	2	8
Calc. Density/g·cm^{-3}	1.87	2.19	2.08
μ /mm^{-1}	10.49	5.90	6.50
F(000)	522	542	3624
Crystal size (mm^3)	0.06 × 0.04 × 0.02	0.39 × 0.24 × 0.20	0.13 × 0.06 × 0.06
2θ range data collection/°	4.9 ÷ 61.2	3.4 ÷ 31.5	3.4 ÷ 28.4
Index ranges	$-12 \le h \le 10$; $-12 \le k \le 12$; $0 \le l \le 12$	$-11 \le h \le 11$; $-15 \le k \le 13$; $0 \le l \le 16$	$-29 \le h \le 28$; $-19 \le k \le 24$; $-28 \le l \le 27$
Reflection collected	3497	5155	17095
Independent reflections	3497 [R_{int} = 0.11]	5155 [R_{int} = 0.04]	17095 [R_{int} = 0.08]
T_{max}, T_{min}	0.813, 0.614	0.247, 0.169	0.985, 0.554
Data/restraints/parameters	3497/36/180	5155/34/260	17095/13/810
Goodness-of-fit on F^2	1.01	1.08	1.02
R_1, wR_2	0.090, 0.257	0.032, 0.082	0.058, 0.103
$\Delta\rho_{max}$, $\Delta\rho_{min}$ / e Å^{-3}	2.29, -1.67	1.58, -2.40	1.59, -1.66
CCDC #	1449678	1449680	1449688

X-ray powder diffraction patterns were collected at room temperature on a Bruker Advance D8 diffractometer using Co-Kα (λ = 1.78897 Å), equipped with a LynxEye detector. The powder diffractograms for the synthesized compound were recorded in the 5 – 95º range of 2θ with a step of 0.019º and a counting time of 0.4 s per step.

Results and Discussion

Three supramolecular isomeric forms of Lu-ATA (ATA = 2-aminoterephthalic acid) coordination frameworks were obtained through the reaction of lutetium(III) nitrate with ATA linker at different temperatures using similar intervals of precursors concentration. Although they share the same compositional characteristics, $\{Lu_2(S)_x(C_8H_6NO_4)_3\}_n$ (S = solvent: H_2O or dimethylformamide, DMF), the crystal structures of these new metal-organic networks reveal temperature-dependent supramolecular isomerism. Using optimized temperature ranges, supramolecular isomers **Lu-ATA@100** and **Lu-ATA@150** were obtained hydrothermally as pure, highly crystalline phases (Figure S2a-b) composed of polyhedra-shaped crystals with sizes ranging from 20 to 500 μm (Figure S4). Consequently, the quality of the crystals isolated hydrothermally allows direct structure solution using single-crystal X-ray diffraction (SCXRD). In contrast to above mentioned compounds, the supramolecular isomeric phase **Lu-ATA@RT,** prepared at room temperature (Figure S3 and S4a,d), is composed of smaller crystals (1–3 μm). The crystal growth in gel media is very useful and widely applied technique for obtaining high quality MOFs' single crystals.[43-48] In order to carry out detailed structural analysis for **Lu-ATA@RT**, the crystal growth in TMOS gel media has been applied. After one week in gel-phase, the yellow dendritically-organized crystals were formed and used for further SCXRD characterization (Figure S1a).

Single crystal X-ray diffraction analysis of **Lu-ATA@RT** reveals that this coordination polymer of formula $\{Lu_2(H_2O)_4(C_8H_5NO_4)_3 \cdot 4H_2O\}_n$ crystalizes in a triclinic space group *P*-1 with unit cell parameters summarized in Table 1. The asymmetric unit of **Lu-ATA@RT** contains one lutetium atom, one and half aminoterephthalic acid (ATA), two coordinated and two crystallization water molecules (Figure S6).

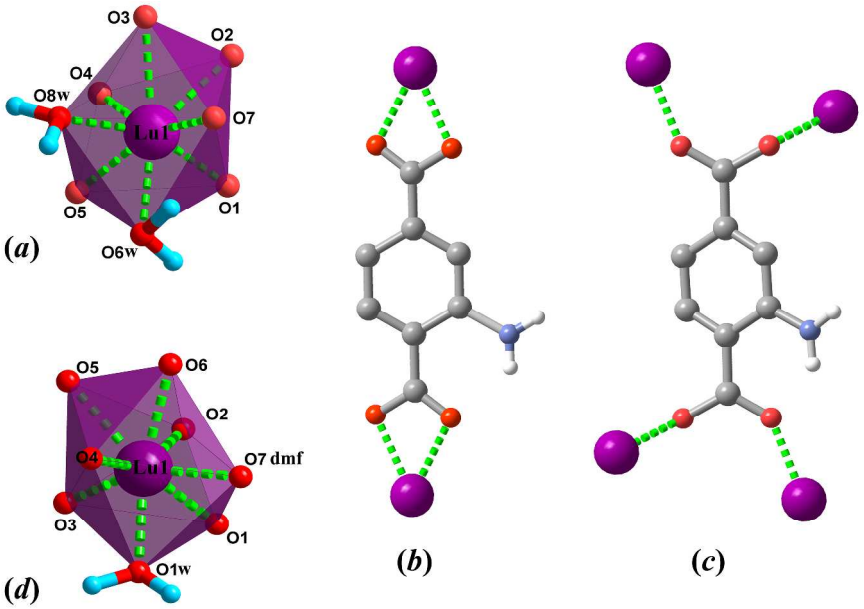

Scheme 1. Coordination environment of Lu(III) ion in (a) **Lu-ATA@RT** and (d) **Lu-ATA@100** polymorphs, and coordination modes of the 2-aminoterephtalic ligand (b) μ -(η_2 : η_2) and (c) μ_4 -(η_1 : η_1 : η_1 : η_1) in both frameworks. Hydrogen atoms of benzene ring were omitted for clarity. Lutetium atoms are depicted as violet spheres.

As shown in Scheme 1a, the lutetium center adopts a distorted bicapped trigonal prismatic geometry and is surrounded by eight oxygen atoms where six of them belong to four carboxylic groups of ATA ligands and two to coordinated water molecules. In the structure of **Lu-ATA@RT**, the 2-aminoterephthalic acid (ATA) exhibits two different tetradentate coordination modes (Scheme 1b-c): the mode (b) μ -(η_2 : η_2), where two oxygen atoms of one carboxylic group chelate one lutetium ion; the mode (c) μ_4 -(η_1 : η_1 : η_1 : η_1), where the aminoterephthalate dianion coordinates four lutetium centers by each available oxygen atoms proceeding from two

carboxylate groups. Consequently, ATA ligands in μ -(η_2 : η_2) and μ_4 -(η_1 : η_1 : η_1 : η_1) coordination modes link lutetium ions in alternately manner to form one-dimensional (1D) chains of Lu polyhedra extended along the *b*-crystallographic direction and arranging into the two-dimensional (2D) substructure of the **Lu-ATA@RT** framework (Figure S7d). Additionally, the ATA ligands behaving only in μ -(η_2 : η_2) mode link lutetium ions in parallel mode and define a second 2D substructure of **Lu-ATA@RT** (Figure S7e). Such 2D-substructures are further associated together through the angular coordination to Lu polyhedra chain resulting in a 3D framework with large rhombohedral channels running along *a*- and *b*-crystallographic axis (Figure 1a-b).

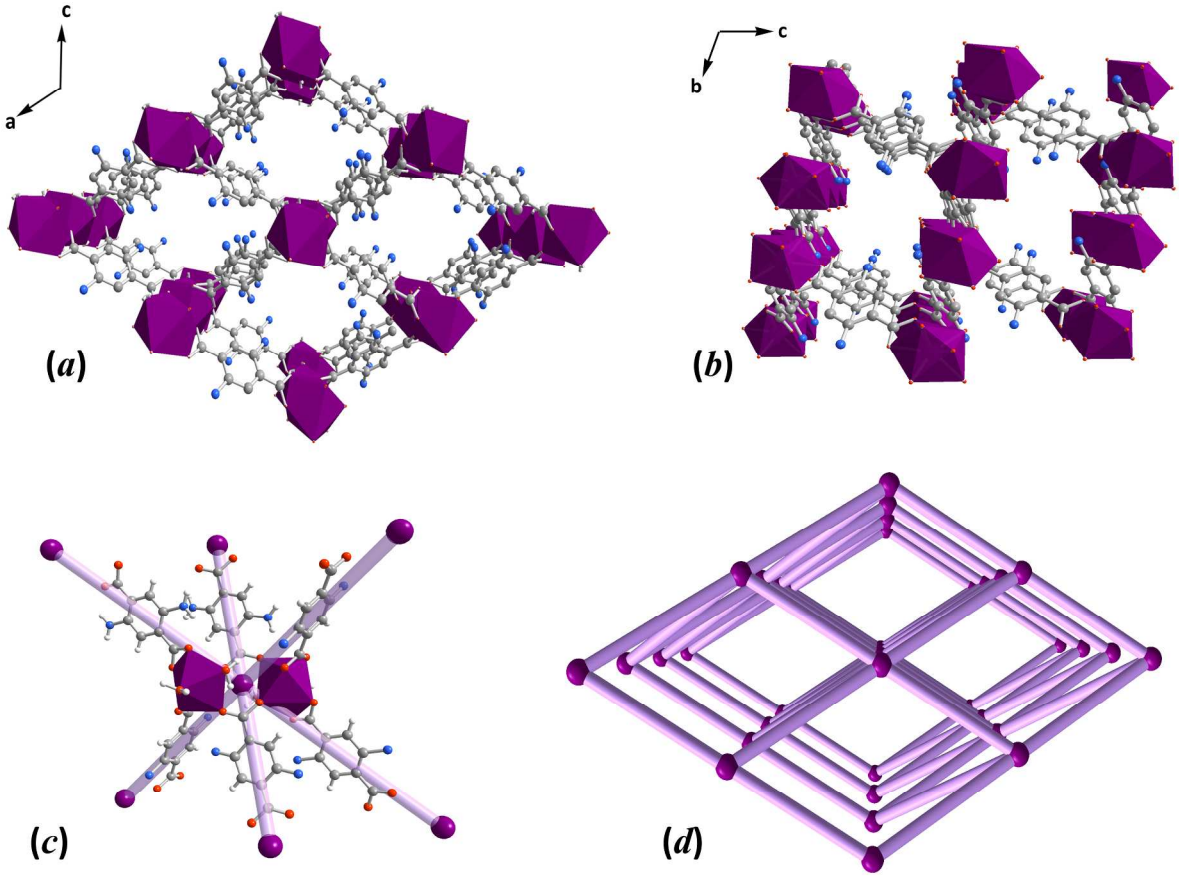

Figure 1. Representation of 3D polymeric structure of **Lu-ATA@RT** that possesses large rhombohedral channels: views (a) along *b*-axis and (b) along *a*-axis. (c) The dinuclear lutetium

motif acted as SBU with linear ATA connectors, and (d) the topological representation of **pcu** simple net of **Lu-ATA@RT**.

According to the void analysis performed with PLATON program,[49] using a probe molecule radius of 1.4 Å and a grid interval of 0.2 Å, the extended 3D structure of **Lu-ATA@RT** framework possess 150 $Å^3$ (15.8 %) of free void space. It is worth noting that the structure of **Lu-ATA@RT** supramolecular isomer is formed by a dinuclear lutetium motif acting as elementary structural building unit (SBU) and can be defined as a simple node during the topological analysis of the framework (Figure 1c). Thus, according to the analysis performed by TOPOSPro,[50] the resulting 3D arrangement corresponds to a 6-connected uninodal net of **pcu** alpha-Po primitive cubic type with ($4^{12}.6^3$) point (Schläfli) symbol (Figure 1d), where the dinuclear lutetium motif act as a nodes and ATA ligands as a bidentate rods.

Compound **Lu-ATA@100,** with formula $\{Lu_2(H_2O)_2(C_3H_7NO)_2(C_8H_5NO_4)_3\}_n$, crystallizes in a triclinic space group *P*-1 with unit cell parameters summarized in Table 1. The asymmetric unit of **Lu-ATA@100** is composed of one lutetium atom, one and a half aminoterephthalic acid (ATA), one coordinated water and one coordinated DMF molecules (Figure S8). The coordination environment of lutetium ion in **Lu-ATA@100** is formed by eight oxygen atoms, where six of them (O1−O6) belong to three carboxylic groups of ATA ligands, one (O1w) to coordinated water and one (O7dmf) to coordinated DMF molecules, and adopts a distorted bicapped trigonal prismatic geometry (Scheme 1d). Notably, in **Lu-ATA@100**, the 2-aminoterephthalic acid (ATA) structure exhibits same (b) μ -(η_2 : η_2) and (c) μ_4 -(η_1 : η_1 : η_1 : η_1) coordination modes (Scheme 1b-c) as in **Lu-ATA@RT** structure. However, the ATA linker behaving in μ_4–mode bridges two nearest metal centers, forming a dimeric lutetium unit as shown in Figure 2a.

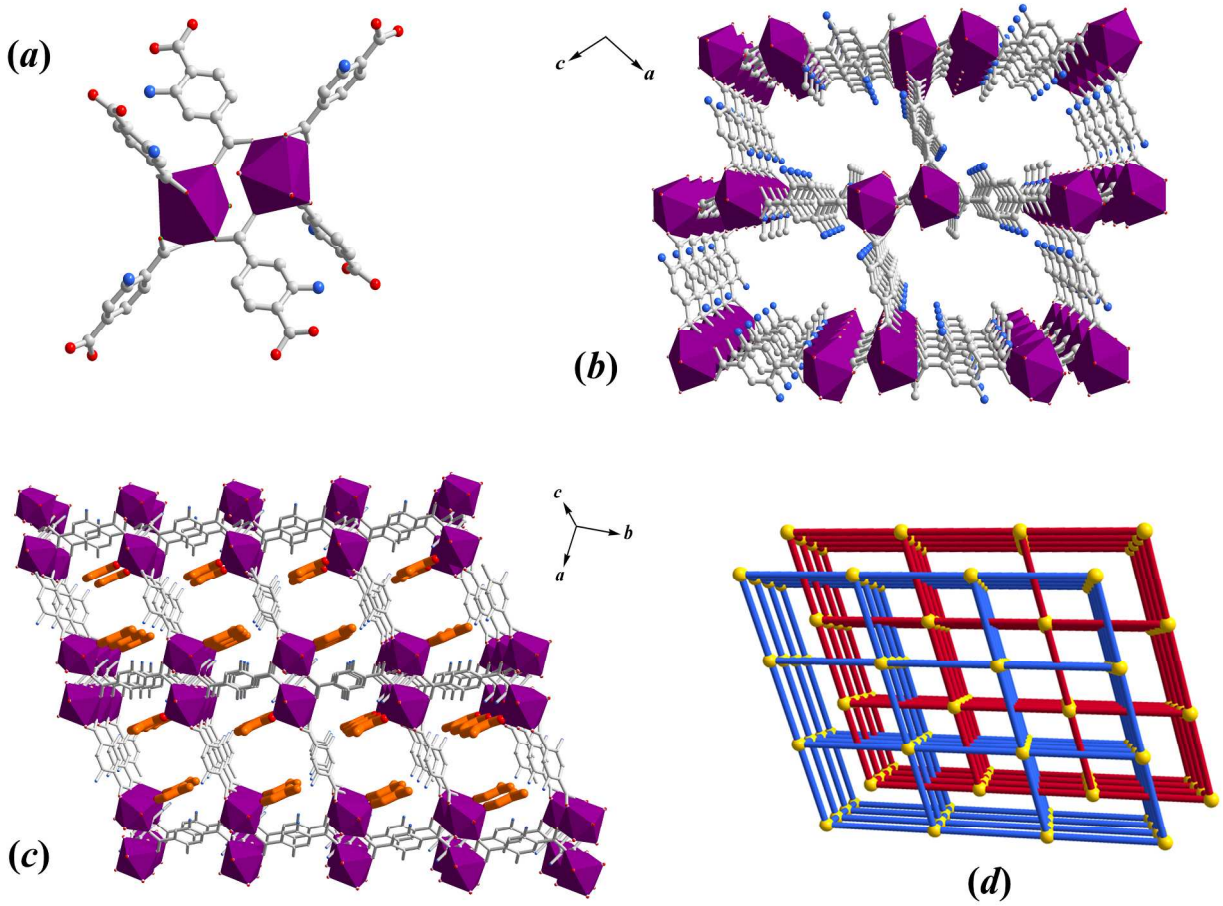

Figure 2. (a) Dimeric lutetium structural unit that forms the 3D extended framework of **Lu-ATA@100** with (b) large rhombic channels running along *b*-axis. (c) View along [111] direction of **Lu-ATA@100** showing the coordinated DMF molecules (orange units) pointed into the channels' of the frame. (d) The simplified representation of **Lu-ATA@100** network of **pcu** topological type with interpenetration.

Such secluded lutetium dimers are linked through μ_4–bridging ATA linkers to give a 1D substructure (Figure S9). Furthermore, adjacent chains are further associated together *via* the linear ATA exhibiting μ–chelation, resulting in a 3D framework. As shown in Figure 2b-c, the polymeric network of **Lu-ATA@100** possesses open rhombohedral channels running along *b*-axis. Notably, the coordinated DMF molecules of dimeric lutetium units pointing into channels restrict the aperture of the framework in the [111] direction (Figure 2c). The void analysis performed by PLATON[49] using a probe molecule radius of 1.4 Å and a grid interval of 0.2 Å reveals that **Lu-ATA@100** framework not possess externally accessible surface volume due to

interpenetration as has been proved below. According to the topological analysis, **Lu-ATA@100** framework is a uninodal six-connected net of **pcu** alpha-Po primitive cubic type expressed by ($4^{12}.6^3$) point (Schläfli) symbol. Moreover, the framework structure consists of two independent simple nets of **pcu** topology with the interpenetration belonging to the class Ia,[51] where each net are symmetry-equivalent and related both by translation vector [100] and inversion (Figure 1d). Although an increase of the densities of the obtained Lu-ATA supramolecular isomers with temperature was observed, **Lu-ATA@100** showed an out-of-trend result due to network interpenetration.

The hydrothermal synthesis of **Lu-ATA@150** supramolecular isomer resulted in a dense hexagonally-packed framework structure. As revealed by single crystal X-ray diffraction, the **Lu-ATA@150** of formula $\{Lu_2(C_3H_7NO)(C_8H_5NO_4)_3\}_n$ crystalizes in monoclinic space group *P*21/*a* with unit cell parameters given in Table 1. The asymmetric unit of **Lu-ATA@150** contains four crystallographically independent lutetium atoms, six aminoterephthalic acid (ATA) and two coordinated DMF molecules (Figure S10). Three lutetium ions (Lu1, Lu3 and Lu4) adopt a distorted monocapped trigonal prismatic coordination geometry (Scheme 2a-c,d) by participation of seven oxygen atoms: (a), (c) all of them from carboxylate groups of ATA ligands (Lu1 and Lu3 centers); (d) six from carboxylate groups of ATA ligands and one (O26dmf) from coordinated DMF molecule (Lu4 center).

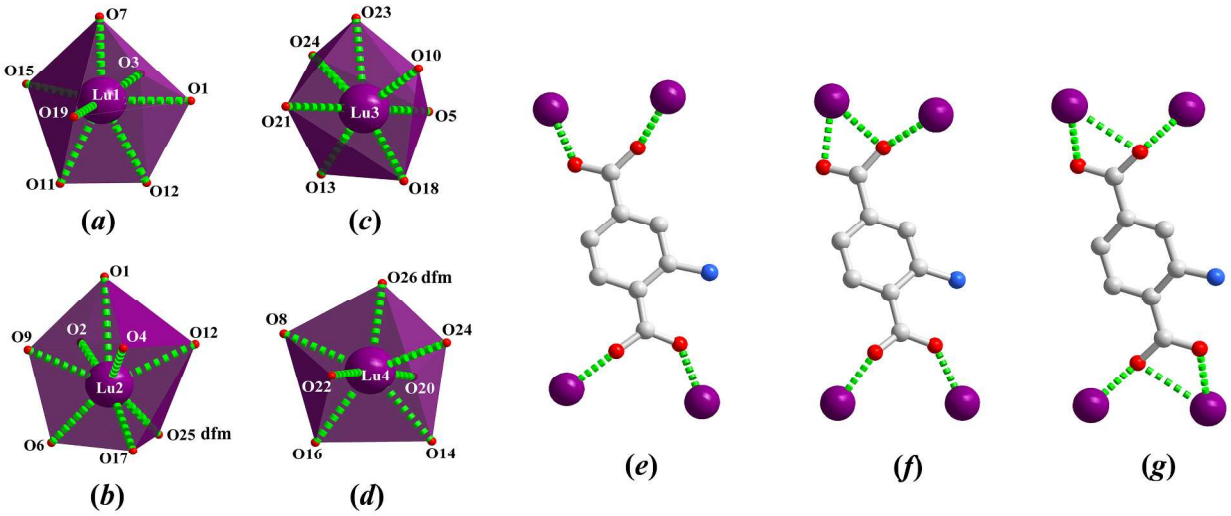

Scheme 2. Coordination environments of four Lu(III) ions in **Lu-ATA@150** with corresponding atom labeling scheme: (a) and (c)–(d) monocapped and (b) bicapped trigonal truncated prisms. The coordination modes of the 2-aminoterephthalic ligands: (e) μ_4 -(η_1 : η_1 : η_1 : η_1), (f) μ_4 -(η_1 : η_1 : η_1 : η_2), (e) μ_4 -(η_1 : η_2 : η_1 : η_2) in **Lu-ATA@150**. Hydrogens were omitted for clarity and lutetium atoms are depicted as violet spheres.

The coordination environment of central lutetium atom Lu2 consists of a distorted bicapped trigonal prismatic geometry comprising eight oxygen atoms: seven of them are originated from carboxylate groups of ATA ligands and one (O25dmf) from a coordinated DMF molecule (Scheme 2b). In the structure of the **Lu-ATA@150** supramolecular isomer, the 2-aminoterephthalic acid (ATA) exhibits three different tetradentate coordination modes (Scheme 2e–g): the mode (e) μ_4 -(η_1 : η_1 : η_1 : η_1), where the aminoterephthalate linker coordinates four lutetium centers by each available oxygen atoms from two carboxyl groups; the mode (f) μ_4 -(η_1 : η_1 : η_1 : η_2), where three oxygen atoms of two carboxyl groups coordinate to three lutetium centers and chelate fourth one; the mode (g) μ_4 -(η_1 : η_2 : η_1 : η_2), where each of carboxyl groups coordinates to one lutetium center and chelates the second one.

As seen in Figure 3a, the neighboring lutetium atoms are connected together through the carboxylate groups of ATA ligands (Scheme 2) in (e)–(g) coordination fashions to form an infinite chain of lutetium polyhedra running along crystallographic *b*-axis. Notably, the

polymeric 1D chain consists of two types of dinuclear motifs (Figure 3b-c): (b) edge-sharing and (c) corner-sharing units. Furthermore, the 1D skeleton of lutetium centers are extended by ATA linkers resulting in hexagonally packed 3D supramolecular architecture. As shown in Figure 3d, the polymeric network of **Lu-ATA@150** is a cage-like structure with triangular windows which are partially obstructed by coordinated DMF molecules of 1D lutetium skeleton. The solvent-accessible volume of **Lu-ATA@150** calculated by PLATON[49] is 374.6 $Å^3$ (a probe molecule radius of 1.4 Å and a grid interval of 0.2 Å were used) and corresponds to 6.1 % of the unit cell volume. Moreover, the polymeric network of **Lu-ATA@150** is four-nodal 3,4,4,9-connected net of new topological type with $(4.5^2)_2(4^4.5.6)(4^4.5^2)(4^8.5^{12}.6^{16})_2$ point (Schläfli) symbol (Figure 3e). In the simplification procedure, the dinuclear lutetium motifs act as nine-connected nodes while the ATA ligands as bidentate rods, three-connected and four connected nodes (Figure S11). Interestingly, due to the cage-like structure of **Lu-ATA@150**, the empty space of the network can be represented by tilling with [4 9 11 6] tile transitivity (Figure 3f).

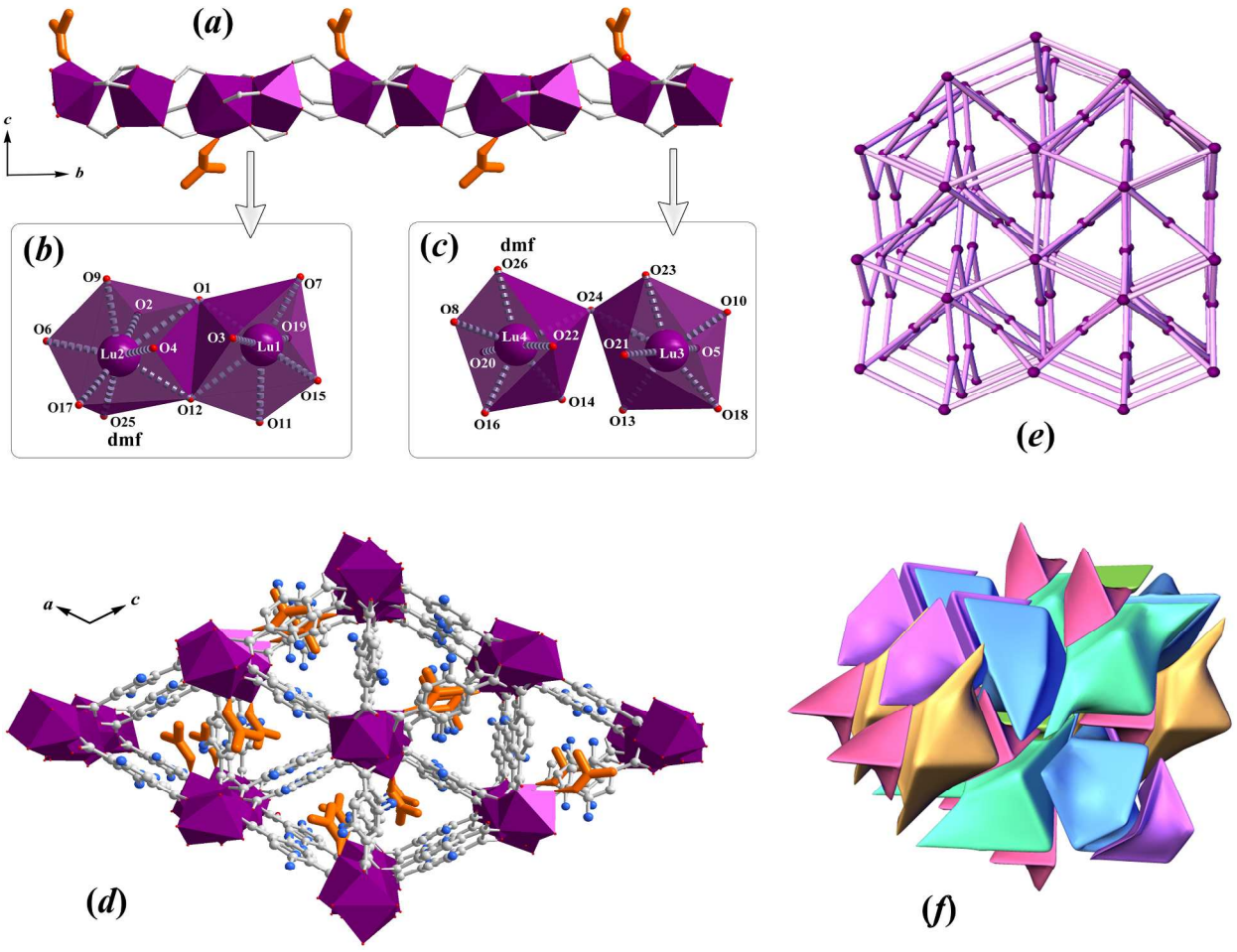

Figure 3. (a) One dimensional chain of lutetium polyhedra in **Lu-ATA@150** composed of two types of dinuclear: (b) edge-sharing and (c) corner-sharing units. Coordinated DMF molecules are drawn in orange. (d) View along *b*-axis to the 3D cage-like framework of **Lu-ATA@150** with triangular windows. (e) The simplified net of **Lu-ATA@150** of new hexagonal-packed topological type and (f) its tilled structure of [4 9 11 6] transitivity.

Thermal stability in air atmosphere of the three Lu-ATA supramolecular isomers was investigated and the thermal decomposition profiles are shown in Figure S12. The degradation of **Lu-ATA@RT** proceeds in two stages, as depicted in Figure S12a. The first mass loss between 30 and 120 °C with a total mass loss of 15.5 % (calculated 14.8 %), corresponds to the simultaneous release of four water molecules trapped in the pores and four coordinated to lutetium atoms, which is accompanied by an endothermic peak in the SDTA curve. Up to 300 °C, the resulted anhydrous compound remains stable until the second stage, which takes place in

the range 320−540 °C (continuous process) with the total mass loss of *ca*. 44.4 %, and corresponds to the progressive decomposition of the organic part of the framework, associated with exothermic peaks in SDTA graph. According to the mass of the remaining solid, the residual product of decomposition is Lu_2O_3

In turn, the thermal decomposition profile of **Lu-ATA@100** shows a different behavior and is composed of two well-separated steps. As shown in Figure S12b, the first mass loss step occurs at higher temperature in the range 170−230 °C with the mass loss of 16.3 % and consists of two contributions which correspond to evacuation of two coordinated water and two DMF molecules (calculated 16.5 %). These processes are conformed by an endothermic peak in SDTA plot. The anhydrous framework of **Lu-ATA@100** remains stable up to 340 °C. The second decomposition stage takes place in the range 350−550 °C with the mass loss of *ca*. 61.2% and attributed to oxidative degradation of the organic part of the polymeric frame, associated with exothermic peaks in SDTA curve.

Similarly, the degradation process for **Lu-ATA@150** supramolecular isomer proceeds in two stages (Figure S12c). The first mass loss between 140 and 230 °C with a mass loss of 7.6 % (calculated 7.3 %), corresponds to the evacuation of two DMF molecules coordinated to lutetium atoms, which is accompanied by an endothermic peak in SDTA curve. In air atmosphere, the anhydrous **Lu-ATA@150** is stable in the 240−320 °C temperature plateau, followed by a second degradation step, which takes place in the range 330−700 °C. The total mass loss of *ca*. 57.3 % corresponds to the decomposition of organic ligands and collapse of the structure (exothermic process).

In order to explore any structural transformation that can take place upon activation of the Lu-ATA isomers and be related to the solvent removal, additional powder X-ray diffraction studies have been performed. As shown in Figures S13 and S14, PXRD patterns of **Lu-ATA@RT** and **Lu-ATA@100** treated in vacuo at 200 C show a loss of crystallinity without any notable structural transformations. In contrast, **Lu-ATA@150** exhibits irreversible structural change upon activation at 200 °C in vacuo, as illustrated in Figure S15. Powder X-ray diffraction patterns of **Lu-ATA@150** desolvated form has been indexed in the triclinic crystal system with the following unit cell dimensions: a = 10.56(2) Å, b = 10.33(2) Å, c = 7.48(1) Å, α = 95.6(1)°, β = 109.2(1)°, γ = 113.3(2)°, V = 683(2) Å^3. The results reveal that the unit cell contracts after desolvation process lowering the crystal symmetry to *P*-1.

The porosity of the three supramolecular isomers could not be studied with nitrogen physisorption due to the very narrow porosity that these materials exhibit. That fact, in combination with the big crystal size led to diffusional problems and made carbon dioxide adsorption a suitable choice for their textural characterization as it has been proposed several times in literature.[52] The adsorption of carbon dioxide on the series of materials was analyzed at 273 K at low and high pressure.

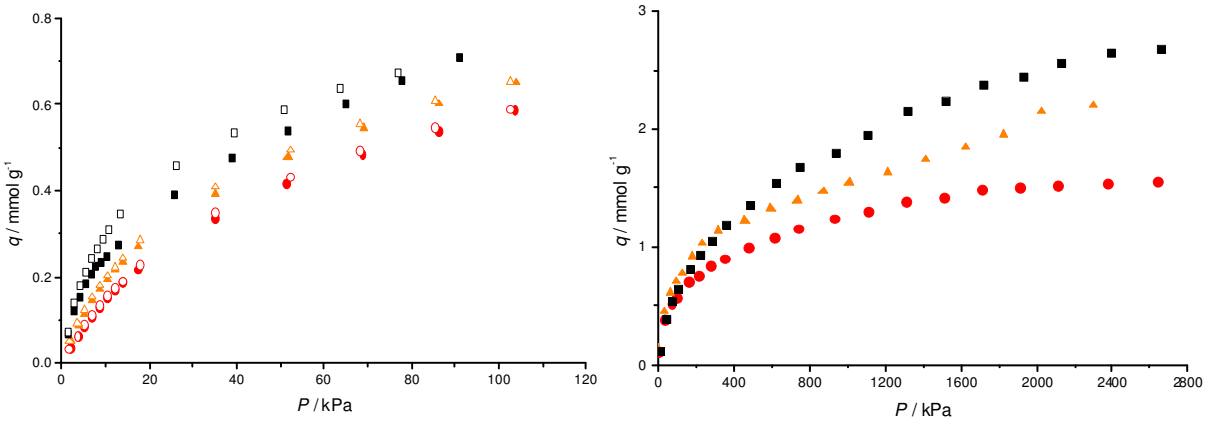

Figure 4. Carbon dioxide adsorption at 273 K at low (left) and high pressure (right) in **Lu-ATA@RT** (black squares), **Lu-ATA@100** (orange triangles) and **Lu-ATA@150** (red circles). Full and empty symbols represent adsorption and desorption, respectively. The amount of CO_2 adsorbed is designated as *q*.

At carbon dioxide pressure up to 100 kPa **Lu-ATA@RT**, **Lu-ATA@100** and **Lu-ATA@150** adsorb a similar amount, around 0.7, 0.65 and 0.59 mmol/g respectively. It is important to notice that the removal of coordinated DMF molecules, which restricts the accessibility to vacant pore space in **Lu-ATA@100** and **Lu-ATA@150** frameworks, is essential to obtain adsorption of carbon dioxide. When the pretreatment was carried out at 323 K the materials did not show any uptake, in contrast the porosity was accessible if temperatures higher than 373 K were applied to pretreat the samples. At higher pressures the same trend is confirmed, being **Lu-ATA@150** the material with lower adsorption capacity with a maximum value of 1.56 mmol/g at 2636 kPa. **Lu-ATA@100** adsorbs a higher amount reaching 2.2 mmol/g at 2299 kPa. The material with the highest adsorption capacity for carbon dioxide of the supramolecular isomers series is **Lu-ATA@150**, adsorbing a maximum of 2.7 mmol/g at 2656 kPa. The adsorption trend of the three supramolecular isomers is in agreement with the obtained pore volumes from the crystallographic information, exhibiting the three of them a very narrow porosity.

The optical properties of the Lu-ATA MOFs series were analyzed by light absorption and fluorescence spectroscopy. The three isomeric structures show fluorescence emission in solid state as well as in suspension of acetonitrile and toluene (Table 2). Lu(III) has full *f* orbitals and thus the typical lanthanide metal luminescence cannot occur. The band at longest wavelength in the free linker, assigned to a highest occupied molecular orbital to lowest unoccupied molecular orbital (HOMO-LUMO) transition with a $n \rightarrow \pi^*$ nature,[53, 54] appears in the MOFs' spectra without important shifts. This seems to indicate that the contribution of the metal orbitals to the

frontier orbitals might be negligible and that this transition remains linker based in the MOFs.[54, 55] Nevertheless, computational studies are needed to gain insights on the location of HOMO and LUMO in each Lu-ATA system and thus to confirm if the bands around 370-380 nm arise form linker based or metal-to-linker charge-transfer (MLCT) transitions.[56-59]

Table 2. Absorption (λ_{abs}) and emission (λ_{em}) maxima along with derived Stokes shifts for studied supramolecular isomers **Lu-ATA@RT**, **Lu-ATA@100** and **Lu-ATA@150**.

	Compound	λ_{abs} (nm)	λ_{em} (nm)	Stokes shift (nm)
Activated powder	**Lu-ATA@RT**	377 (br)	456	79
	Lu-ATA@100	386 (br)	460	79
	Lu-ATA@150	384 (br)	456	70
Toluene	**Lu-ATA@RT**	378	448	70
	Lu-ATA@100	380	450	70
	Lu-ATA@150	385	451	66
Acetonitrile	**Lu-ATA@RT**	366	430	64
	Lu-ATA@100	379	440	61
	Lu-ATA@150	387	450	63
	Linker ester	367	428	61

(br) = broad signal

Of particular interest is the trend observed in both the absorption and the emission maxima of the different Lu-ATA supramolecular isomers in acetonitrile (Figure 5), which is not observed in the powder or in suspension of an unipolar solvent like toluene (Supporting Information S16-S21). The spectra exhibit a clear hypsochromic shift of 10 nm step following the order **Lu-ATA@RT < Lu-ATA@100 < Lu-ATA@150**.

It is known that increasing the polarity of the solvent leads to blue shifts in nπ* transitions.[60] In the ground state, the dipoles of the solvent are oriented with their positive endings towards the n

orbital bearing the lone pair of electrons. Upon excitation the n orbital losses electron density (which is injected into the π*) but the solvent dipoles do not switch in this timescale and thus a repulsive effect between the solvent molecules and the electron-poor nitrogen destabilizes the excited state.

Thus a possible explanation for the different blue shift of each Lu-ATA MOF suspended in acetonitrile compared to the corresponding spectra in powder and in toluene could be that the polar solvent molecules interact with a different strength with each supramolecular isomer, thus leading to different degrees of destabilization of their excited state. That is, solvatochromism[55, 61] might be different for each Lu-ATA structure. Nevertheless, MOFs can undergo several mechanisms that lead to optical changes[62] and further studies would be required to unequivocally explain this trend.

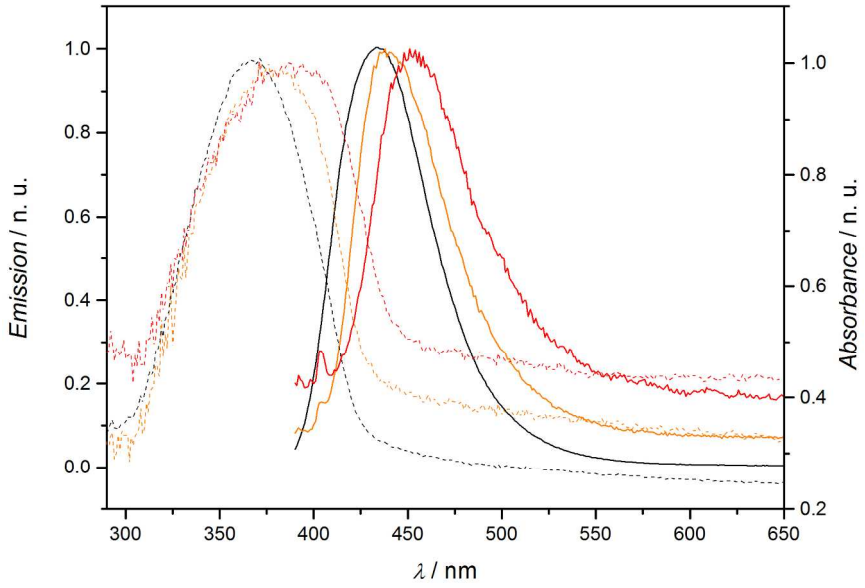

Figure 5. Absorption (dashed lines) and emission (solid line) spectra of **Lu-ATA@RT** (black), **Lu-ATA@100** (orange), and **Lu-ATA@150** (red) in acetonitrile suspension ($5 \cdot 10^{-2}$ g/L). Bands are normalized for better visualization. The non-zero backgrounds results from light scattering.

Conclusions

Three supramolecular isomeric forms of lutetium-based MOF, **Lu-ATA@RT**, **Lu-ATA@100** and **Lu-ATA@150**, built by 2-aminoterephthalic linker were synthesized starting from the same precursors. The structure of the final isomeric form of Lu-ATA framework as well as its crystal packing is influenced by the temperature applied during the synthesis. Thus, the room temperature approach leads to formation of **Lu-ATA@RT** framework having **pcu** topology while the synthesis at 100 ºC results in **Lu-ATA@100** forming an interpenetrated (class Ia) analogue of the **pcu**-net. A dense cage-like structure with a new topology is formed at 150 ºC under hydrothermal conditions (**Lu-ATA@150**). Notably, the structural differences between three supramolecular isomers of Lu-ATA MOF expressed by general formula of $\{Lu_2(S)_x(ATA)_3\}_n$ are reflected on their absorption behaviour towards CO_2. High-pressure CO_2 absorption results reveal that the three Lu-ATA supramolecular isomers possess narrow porosity, the maximum capacity follows the trend **Lu-ATA@RT > Lu-ATA@100 > Lu-ATA@150,** in agreement with the calculated pore volumes extracted from the crystallographic information. Lu-ATA series suspended in acetonitrile exhibited a blue shift of different magnitude in their absorption and emission bands compared to the spectra in toluene or in powder, which might be an indication of different solvation efficiency in the diverse structures.

ASSOCIATED CONTENT

Supporting Information. Optical and electron microscopy images for Lu-ATA polymorphs, additional structure images, PXRD of synthesized materials, TG/SDTA data plots, additional

absorption and emission spectra. This material is available free of charge via the Internet at http://pubs.acs.org.

The supplementary crystallographic data for this paper were deposited to Cambridge Crystallographic Data Centre with CCDC numbers of 1449678, 1449680 and 1449688. These data can be obtained free of charge via www.ccdc.cam.ac.uk/data_request/cif, or by emailing data_request@ccdc.cam.ac.uk, or by contacting The Cambridge Crystallographic Data Centre, 12, Union Road, Cambridge CB2 1EZ, UK; fax: +44 1223 336033.

AUTHOR INFORMATION

Corresponding Author

*Corresponding authors emails: P.SerraCrespo@tudelft.nl and J.Gascon@tudelft.nl

Author Contributions

‡These authors contributed equally. The manuscript was written through contributions of all authors. All authors have given approval to the final version of the manuscript.

Funding Sources

The research leading to these results has received funding from the European Research Council under the European Union's Seventh Framework Programme (FP/2007-2013) / ERC Grant Agreement n. 335746, CrystEng-MOF-MMM

ACKNOWLEDGMENT

S.G.-G and R. M.-M. thank to Ministerio de Economía y Competitividad, MAT2013-40950-R, for financial support.

ABBREVIATIONS

MOF, metal-organic framework; **ATA**, 2-aminoterephthalic acid; **DMF**, N,N´-dimethylformamide; **RT**, room temperature; **SEM**, scanning electron microscopy; **SCXRD**, single-crystal X-ray diffraction; **SBU**, structural building unit; **SDTA**, simultaneous difference thermal analysis; **HOMO**, highest occupied molecular orbital; **LUMO**, lowest unoccupied molecular orbital; **MLCT**, metal-to-linker charge-transfer; **CCDC**, Cambridge crystallographic data center.

REFERENCES

(1) Rowsell, J. L. C.; Yaghi, O. M., *Microporous Mesoporous Mater.* **2004,** 73, 3-14.
(2) Long, J. R.; Yaghi, O. M., *Chem. Soc. Rev.* **2009,** 38, 1213-1214.
(3) Hoskins, B. F.; Robson, R., *J. Am. Chem. Soc.* **1990,** 112, 1546-1554.
(4) Kuppler, R. J.; Timmons, D. J.; Fang, Q.-R.; Li, J.-R.; Makal, T. A.; Young, M. D.; Yuan, D.; Zhao, D.; Zhuang, W.; Zhou, H.-C., *Coord. Chem. Rev.* **2009,** 253, 3042-3066.
(5) Li, J.-R.; Kuppler, R. J.; Zhou, H.-C., *Chem. Soc. Rev.* **2009,** 38, 1477-1504.
(6) Corma, A.; Garcia, H.; Llabres i Xamena, F. X., *Chem. Rev.* **2010,** 110, 4606-4655.
(7) Meek, S. T.; Greathouse, J. A.; Allendorf, M. D., *Adv. Mater.* **2011,** 23, 249-267.
(8) Horcajada, P.; Gref, R.; Baati, T.; Allan, P. K.; Maurin, G.; Couvreur, P.; Férey, G.; Morris, R. E.; Serre, C., *Chem. Rev.* **2011,** 112, 1232-1268.
(9) O'Keeffe, M.; Yaghi, O. M., *Chem. Rev.* **2011,** 112, 675-702.
(10) Yaghi, O. M.; O'Keeffe, M.; Ockwig, N. W.; Chae, H. K.; Eddaoudi, M.; Kim, J., *Nature* **2003,** 423, 705-714.
(11) Zhou, H.-C.; Long, J. R.; Yaghi, O. M., *Chem. Rev.* **2012,** 112, 673-674.
(12) Schubert, U., *Chem. Soc. Rev.* 40, 575-582.
(13) Seoane, B.; Castellanos, S.; Dikhtiarenko, A.; Kapteijn, F.; Gascon, J., *Coord. Chem. Rev.* **2016,** 307, Part 2, 147-187.
(14) Furukawa, H.; Cordova, K. E.; O'Keeffe, M.; Yaghi, O. M., *Science* **2013,** 341.
(15) Aakeroy, C. B.; Champness, N. R.; Janiak, C., *CrystEngComm* **2010,** 12, 22-43.
(16) Hennigar, T. L.; MacQuarrie, D. C.; Losier, P.; Rogers, R. D.; Zaworotko, M. J., *Angew. Chem., Int. Ed.* **1997,** 36, 972-973.
(17) Moulton, B.; Zaworotko, M. J., *Chem. Rev.* **2001,** 101, 1629-1658.
(18) Monge, A.; Gandara, F.; Gutierrez-Puebla, E.; Snejko, N., *CrystEngComm* **2011,** 13, 5031-5044.
(19) Shi, F.-N.; Ananias, D.; Yang, T.-H.; Rocha, J., *J. Solid State Chem.* **2013,** 204, 321-328.
(20) Yan, Z.; Li, M.; Gao, H.-L.; Huang, X.-C.; Li, D., *Chem. Commun.* **2012,** 48, 3960-3962.
(21) Santra, A.; Bharadwaj, P. K., *Cryst. Growth Des.* **2014,** 14, 1476-1485.
(22) Frahm, D.; Hoffmann, F.; Fröba, M., *Cryst. Growth Des.* **2014,** 14, 1719-1725.
(23) Kumalah, S. A.; Holman, K. T., *Inorg. Chem.* **2009,** 48, 6860-6872.
(24) Bon, V.; Senkovska, I.; Baburin, I. A.; Kaskel, S., *Cryst. Growth Des.* **2013,** 13, 1231-1237.

(25) Zhu, N.; Lennox, M. J.; Duren, T.; Schmitt, W., *Chem. Commun.* **2014,** 50, 4207-4210.
(26) Katsenis, A. D.; Puškarić, A.; Štrukil, V.; Mottillo, C.; Julien, P. A.; Užarević, K.; Pham, M.-H.; Do, T.-O.; Kimber, S. A. J.; Lazić, P.; Magdysyuk, O.; Dinnebier, R. E.; Halasz, I.; Friščić, T., *Nat Commun* **2015,** 6.
(27) Jeong, S.; Kim, D.; Shin, S.; Moon, D.; Cho, S. J.; Lah, M. S., *Chem. Mater.* **2014,** 26, 1711-1719.
(28) Konstas, K.; Taupitz, K. F.; Turner, D. R.; Kennedy, D. F.; Hill, M. R., *CrystEngComm* **2014,** 16, 8937-8940.
(29) Cheetham, A. K.; Rao, C. N. R.; Feller, R. K., *Chem. Commun.* **2006**, 4780-4795.
(30) Kieslich, G.; Kumagai, S.; Butler, K. T.; Okamura, T.; Hendon, C. H.; Sun, S.; Yamashita, M.; Walsh, A.; Cheetham, A. K., *Chem. Commun.* **2015,** 51, 15538-15541.
(31) Canadillas-Delgado, L.; Fabelo, O.; Pasan, J.; Deniz, M.; Martinez-Benito, C.; Diaz-Gallifa, P.; Martin, T.; Ruiz-Perez, C., *Acta Crystallogr., Sect. B* **2014,** 70, 19-27.
(32) Liu, G.-X.; Xu, H.; Zhou, H.; Nishihara, S.; Ren, X.-M., *CrystEngComm* **2012,** 14, 1856-1864.
(33) Aulakh, D.; Varghese, J. R.; Wriedt, M., *Inorg. Chem.* **2015,** 54, 8679-8684.
(34) Rybak, J.-C.; Tegel, M.; Johrendt, D.; Mueller-Buschbaum, K., *Z. Kristallogr. - Cryst. Mater.* **2010,** 225, 187-194.
(35) Gándara, F.; de la Peña-O'Shea, V. A.; Illas, F.; Snejko, N.; Proserpio, D. M.; Gutiérrez-Puebla, E.; Monge, M. A., *Inorg. Chem.* **2009,** 48, 4707-4713.
(36) Baburin, I. A.; Leoni, S., *CrystEngComm* **2010,** 12, 2809-2816.
(37) Schroeder, C. A.; Baburin, I. A.; van Wuellen, L.; Wiebcke, M.; Leoni, S., *CrystEngComm* **2013,** 15, 4036-4040.
(38) Almáši, M.; Zeleňák, V.; Opanasenko, M.; Císařová, I., *Catalysis Today* **2015,** 243, 184-194.
(39) Roesky, P. W.; Bhunia, A.; Lan, Y.; Powell, A. K.; Kureti, S., *Chem. Commun.* **2011,** 47, 2035-2037.
(40) Altomare, A.; Cascarano, G.; Giacovazzo, C.; Guagliardi, A.; Burla, M. C.; Polidori, G.; Camalli, M., *J. Appl. Crystallogr.* **1994,** 27, 435.
(41) Sheldrick, G., *Acta Crystallogr., Sect. C.* **2015,** 71, 3-8.
(42) Parkin, S.; Moezzi, B.; Hope, H., *J. Appl. Crystallogr.* **1995,** 28, 53-56.
(43) Henisch, H. K., *Crystal Growth in Gels*. ed.; Dover Publications: 1996.
(44) Yaghi, O. M.; Li, G.; Li, H., *Chem. Mater.* **1997,** 9, 1074-1076.
(45) Petrova, R. I.; Patel, R.; Swift, J. A., *Cryst. Growth Des.* **2006,** 6, 2709-2715.
(46) Foster, J. A.; PiepenbrockMarc-Oliver, M.; Lloyd, G. O.; Clarke, N.; HowardJudith, A. K.; Steed, J. W., *Nat Chem* **2010,** 2, 1037-1043.
(47) Li, H.; Fujiki, Y.; Sada, K.; Estroff, L. A., *CrystEngComm* **2011,** 13, 1060-1062.
(48) Kumar, D. K.; Steed, J. W., *Chem. Soc. Rev.* **2014,** 43, 2080-2088.
(49) Spek, A., *Acta Crystallogr., Sect. D* **2009,** 65, 148-155.
(50) Blatov, V. A.; Shevchenko, A. P.; Proserpio, D. M., *Cryst. Growth Des.* **2014,** 14, 3576-3586.
(51) Baburin, I. A.; Blatov, V. A.; Carlucci, L.; Ciani, G.; Proserpio, D. M., *J. Solid State Chem.* **2005,** 178, 2452-2474.
(52) Lozano-Castelló, D.; Cazorla-Amorós, D.; Linares-Solano, A., *Carbon* **2004,** 42, 1231-1236.

(53) Castellanos, S.; Sai Sankar Gupta, K. B.; Pustovarenko, A.; Dikhtiarenko, A.; Nasalevich, M.; Atienzar, P.; García, H.; Gascon, J.; Kapteijn, F., *Eur. J. Inorg. Chem.* **2015,** 2015, 4648-4652.
(54) Sun, D.; Fu, Y.; Liu, W.; Ye, L.; Wang, D.; Yang, L.; Fu, X.; Li, Z., *Chem. Eur. J.* **2013,** 19, 14279-14285.
(55) Cui, J.; Li, Y.; Guo, Z.; Zheng, H., *Chem. Commun.* **2013,** 49, 555-557.
(56) Hendon, C. H.; Tiana, D.; Fontecave, M.; Sanchez, C.; D'arras, L.; Sassoye, C.; Rozes, L.; Mellot-Draznieks, C.; Walsh, A., *J. Am. Chem. Soc.* **2013,** 135, 10942-10945.
(57) Flage−Larsen, E.; Røyset, A.; Cavka, J. H.; Thorshaug, K., *J. Phys. Chem. C* **2013,** 117, 20610-20616.
(58) Kuc, A.; Enyashin, A.; Seifert, G., *J. Phys. Chem. B* **2007,** 111, 8179-8186.
(59) Coudert, F.-X.; Fuchs, A. H., *Coord. Chem. Rev.* **2016,** 307, Part 2, 211-236.
(60) Turro, N. J.; Ramamurthy, V.; Scaiano, J. C., In *Modern Molecular Photochemistry of Organic Molecules*, University Science Books: Sausalito, 2010.
(61) Lu, Z.-Z.; Zhang, R.; Li, Y.-Z.; Guo, Z.-J.; Zheng, H.-G., *J. Am. Chem. Soc.* **2011,** 133, 4172-4174.
(62) Kreno, L. E.; Leong, K.; Farha, O. K.; Allendorf, M.; Van Duyne, R. P.; Hupp, J. T., *Chem. Rev.* **2012,** 112, 1105-1125.

Table of Contents Graphic and Synopsis

Three new porous metal-organic framework (**Lu-ATA@RT**, **Lu-ATA@100** and **Lu-ATA@150**) with general formula of $\{Lu_2(S)_x(ATA)_3\}_n$ (where S = H_2O, DMF; ATA = 2-aminoterephthalic acid) were obtained. The self-assembled systems composed of aminoterephthalate linker and lutetium ions demonstrate a case of temperature-dependent supramolecular isomerism of their crystal structures. Moreover, the difference between these crystalline isomeric forms is reflected on their gas adsorption behavior.

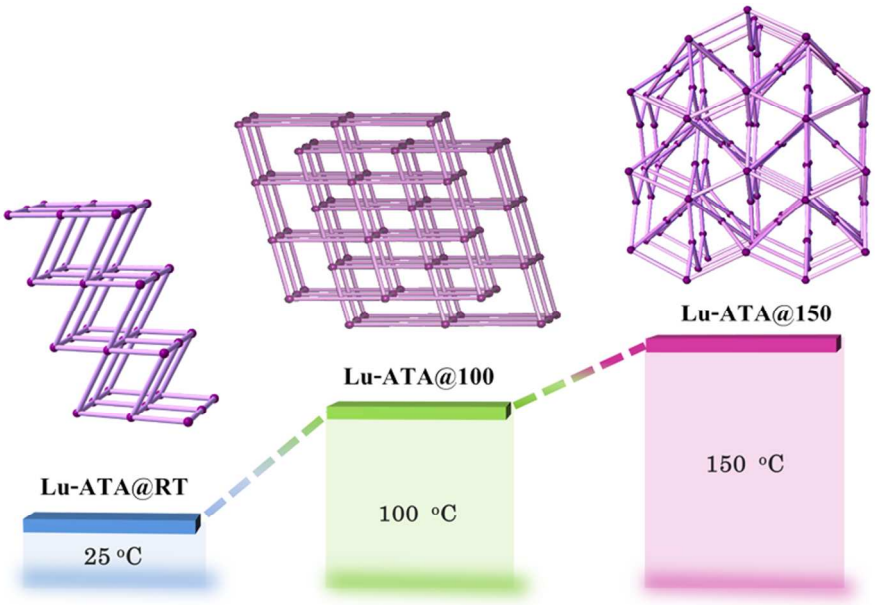
Lu-ATA@RT
25 °C
Lu-ATA@100
100 °C
Lu-ATA@150
150 °C